Ground Motion Activities at DESY – An Overview[*]

C. Montag, BNL, Upton, NY 11973, USA

Abstract

Ground motion studies have been performed at DESY for more than a decade, covering beam motion in the two-ring e-p collider HERA, luminosity preservation in Linear Colliders, and active stabilization methods. An overview of past and present activities will be given.

1 INTRODUCTION

In colliding beams facilities, orbit jitter induced by ground motion is a concern for various reasons. While these machines this jitter may lead to emittance dilution due to nonlinear effects, the dominant effect in machines where both beams experience different magnetic fields is varying relative beam offset at the interaction point (IP), leading to luminosity degradation. Examples of machines where this is the case are two-ring circular colliders (HERA, the B-factories, RHIC, and LHC) and Linear Colliders. At DESY, ground motion studies were started in the late 1980s when HERA was under construction, and continued as part of the two Linear Collider projects SBLC (S-Band Linear Collider) and TESLA.

In this paper, an overview of past and present ground motion studies at DESY is given.

2 CIRCULAR COLLIDERS

During the construction phase of the two-ring e-p collider HERA, the issue of relative IP beam offsets due to ground motion was apparent. Therefore, ground motion effects were studied both theoretically and experimentally. Considering a storage ring of circumference $C = 2\pi R$ composed of N identical FODO cells with identical bends between the quadrupoles, the ratio R_y of vertical closed-orbit distortion amplitude $\hat{y}_c$ to the amplitude $\hat{y}$ of a vertical plane ground wave with wavelength λ can be expressed as [1]

$$
\begin{aligned}
R_y &= \frac{\hat{y}_c}{\hat{y}} \\
&= \frac{\beta_0}{2f} \left\{ \left[\sum_{p=-\infty}^{\infty} J_{4p}\left(\frac{C}{\lambda}\right) C_{4p} \right. \right. \\
&\qquad \left. - J_{4p-2}\left(\frac{C}{\lambda}\right) C_{4p-2} \right]^2 \\
&\qquad + \left[\sum_{p=-\infty}^{\infty} J_{4p-1}\left(\frac{C}{\lambda}\right) C_{4p-1} \right.
\end{aligned}
$$

$$
\left. \left. - J_{4p-3}\left(\frac{C}{\lambda}\right) C_{4p-3} \right]^2 \right\}^{\frac{1}{2}}, \quad (1)
$$

with

$$
\begin{aligned}
C_p &= \frac{(-1)^{p+1}}{\sin\left(\frac{\pi p}{N} - \frac{\mu}{2}\right)} \\
&\quad \cdot \left\{ \sqrt{\hat{\beta}} \cos\left[p\left(\pi\frac{N+1}{N} - \theta_w\right) - \frac{\mu}{2} \right] \right. \\
&\qquad \left. - \sqrt{\check{\beta}} \cos p(\pi - \theta_w) \right\}. \quad (2)
\end{aligned}
$$

Here, μ is the betatron phase advance per FODO cell, θ_w is the direction of incidence of the ground wave with respect to the observation point at $\theta = 0$, β_0 is the β-function at the observation point, and f is the focal length of the quadrupoles. $\hat{\beta}$ and $\check{\beta}$ denote the β-functions in focusing and defocusing quadrupoles, respectively.

The expression for C_p becomes resonant for

$$
|p| = |m|N \pm \nu_y, \quad (3)
$$

where $\nu_y = N\mu/2\pi$ is the vertical tune of the ring. Denoting the distance of ν_y from the closest integer $[\nu_y]$ as $\delta\nu_y$, the maxima of the resonance term $\left|\sin\left(\frac{\pi p}{N} - \frac{\Delta\Phi}{2}\right)\right|^{-1}$ can be expressed as $(\sin\frac{\pi}{N}\delta\nu_y)^{-1}$, which occurs whenever $p = p_{\text{res}} = mN + [\nu_y]$.

The Bessel function J_p differs significantly from zero only for arguments $C/\lambda > p$. Ground waves with $C/\lambda > p_{\text{res}}$ contribute much more to R_y than those with smaller C/λ because all contributions with $p \neq p_{\text{res}}$ are suppressed as seen in Figure 1. Since contributions with $p \neq p_{\text{res}}$ are suppressed due to the resonance condition given above, R_y is small for small values of C/λ and increases in a step-like manner at $C/\lambda = [\nu_y], N - [\nu_y], 2N - [\nu_y], \dots$

After the construction of HERA was completed, several measurements were performed with and without beam to characterize vibration in the operating accelerator environment. The influence of cultural noise of the nearby city of Hamburg was investigated with long-term vibration measurements, Figure 2 [3]. During nights and weekends, the rms vibration amplitude is significantly lower than during working hours, when the traffic is heavier and all kinds of machinery is operated.

As an example of the influence of accelerator operation itself on vibration amplitudes, Figure 3 depicts the vibration signal of a HERA electron quadrupole magnet with and without cooling water flow. As this shows, cooling water flow leads to high-frequency motion.
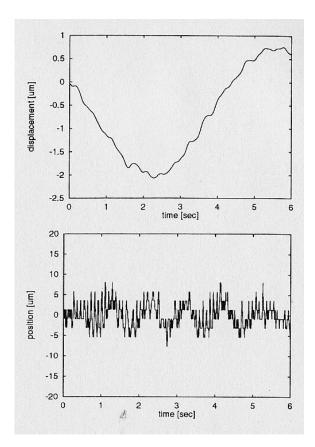
Figure 1: Example of ground motion (upper) and beam orbit jitter (lower), normalized to $\beta = 1\,\mathrm{m}$ [2]. As discussed in the text, the low frequency part of ground motion (the microseismic peak around $1/7$ Hz) is not present in the beam vibration due to its long wavelength of several kilometers.
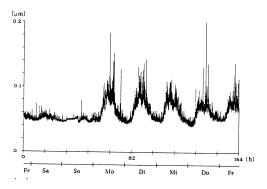

Figure 2: Long term measurement of rms values of vertical ground motion in HERA [3].

3 LINEAR COLLIDERS

In a Linear Collider with its tiny vertical beam dimension of about $\sigma_y \approx 5\,\mathrm{nm}$, ground motion can be a severe performance limitation and may exclude some facility sites entirely. Assuming that the average β-functions $\overline{\beta}$ in the
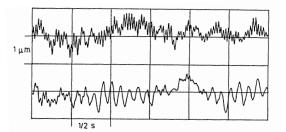

Figure 3: Vertical motion of a quadrupole magnet in the HERA electron ring. Top: cooling water on. Bottom: cooling water off [3].

main linac scale with the square root of the beam energy,

$$\overline{\beta}(s) = \sqrt{\frac{\gamma(s)}{\gamma_{\mathrm{end}}}}\,\overline{\beta}_{\mathrm{end}}, \tag{4}$$

the uncorrelated quadrupole jitter tolerance can then be estimated as [4, 5]

$$\sigma_q = \sqrt{\frac{-2\epsilon_{\mathrm{end}}\overline{\beta}_{\mathrm{end}}\ln\frac{\mathcal{L}}{\mathcal{L}_0}}{N_q}}\cos\frac{\mu}{2}, \tag{5}$$

where ϵ_{end} is the geometric emittance at the end of the main linac, $\overline{\beta}_{\mathrm{end}}$ is the average β-function of the last FODO cell, N_q is the number of quadrupoles per linac, and μ denotes the betatron phase advance per FODO cell. Inserting the appropriate numbers for the SBLC yields an uncorrelated quadrupole jitter tolerance of $\sigma_q = 40\,\mathrm{nm}$.

As SLC experience shows, pulse-to-pulse beam-based orbit correction methods are effective only for frequencies below $f \approx f_{\mathrm{rep}}/25$, where f_{rep} denotes the repetition rate of the collider. In the case of SBLC, $f_{\mathrm{rep}} = 50\,\mathrm{Hz}$; therefore, only beam jitter below $2\,\mathrm{Hz}$ can be suppressed by beam-based methods. This requires that uncorrelated rms vibration amplitudes of the quadrupoles in the main linacs do not exceed $\sigma_q = 40\,\mathrm{nm}$ for frequencies above $f = 2\,\mathrm{Hz}$.

To determine ground motion characteristics at the DESY site, measurements were performed in the HERA tunnel, which can be considered a typical accelerator environment [6]. Figure 4 shows the obtained power spectrum $\Phi(f)$ of vertical ground motion in HERA hall West over a large frequency range.

The corresponding rms amplitude $\sigma_z(f_{\mathrm{lower}})$ for frequencies above a lower frequency limit f_{lower} can be calculated from the power spectrum as

$$\sigma_z(f_{\mathrm{lower}}) = \sqrt{\int_{f_{\mathrm{lower}}}^{\infty}\Phi(f)\,\mathrm{d}f}. \tag{6}$$

This is depicted in Figure 5. To determine correlation properties of ground motion, two sensors were placed at various distances on the floor of HERA hall West. From the simultaneously taken signals $x_1(t)$, $x_2(t)$, the coherence

$$|\gamma(\omega)| = \frac{|\langle p_{12}(\omega)\rangle|}{\sqrt{\langle p_{11}(\omega)\rangle\langle p_{22}(\omega)\rangle}} \tag{7}$$
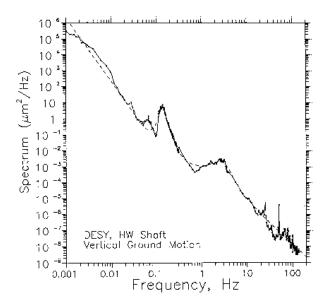
Figure 4: Ground motion power spectrum obtained in HERA hall West. The dashed line shows a fit used for modeling purposes [6].

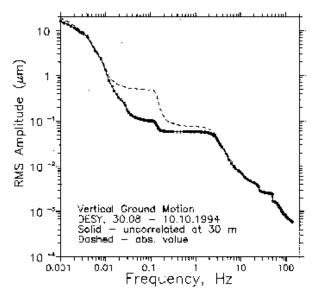Figure 5: rms value of ground motion measured in HERA hall West, calculated by integrating the corresponding spectrum (Figure 4) from f_{lower} to infinity [6]. The obtained rms value is shown as a function of this lower frequency limit f_{lower}.

was determined, with

$$p_{ij}(\omega) = \lim_{T \to \infty} \frac{1}{T} \int_{-\frac{T}{2}}^{\frac{T}{2}} dt \int_{-\frac{T}{2}}^{\frac{T}{2}} dt' x_i(t') x_j(t) e^{i\omega t' - i\omega t}.$$

(8)

Figure 6 shows the resulting coherence of vertical ground motion for distances of 5 m, 15 m, and 30 m. At distances of 15 m and 30 m, the coherence drops rapidly for frequencies above $2 - 3$ Hz. Since the distance between

Figure 6: Coherence spectra of two seismometers separated by 5 m (top), 15 m (middle), and 30 m (bottom), measured in HERA hall West [6]

quadrupoles in a future Linear Collider is similar or even larger, quadrupole motion is expected to be uncorrelated in this frequency band. According to Figure 5, the rms vibration amplitude for frequencies above 2 Hz is about 70 nm. Since this uncorrelated quadrupole vibration is above the tolerance level of $\sigma_q = 40$ nm, active stabilization is required to reduce quadrupole jitter.

An active stabilization system was developed at DESY as part of the SBLC study [7, 8]. A regular linac quadrupole was placed on a piezo actuator, Figure 7. Vertical magnet vibration was detected by a geophone on top of the quadrupole. The output signal from this sensor was processed by a PC with an A/D board, and an appropriate correction signal was sent to the actuator to keep the magnet's center at rest. The resulting feedback gain of this system, Figure 8, resulted in a vertical rms vibration amplitude of 25 nm for frequencies above 2 Hz even in a very noisy environment with a corresponding ground motion rms amplitude of 95 nm, Figure 9.

In the case of TESLA, long bunch trains of about 1000 bunches and large bunch spacing of $1\,\mu$sec allow for fast beam-based bunch-to-bunch orbit correction, making additional stabilization efforts unnecessary. This scheme utilizes the beam-beam deflection at the interaction point to
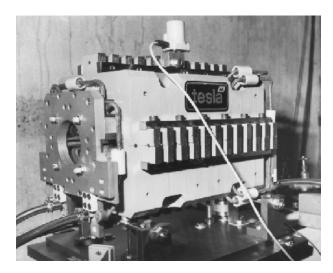
Figure 7: Active stabilization system, consisting of a geophone on top of the magnet and a piezo actuator below it to tilt the quadrupole around its horizontal transverse axis in order to keep its center at rest [7, 8]. The length of the magnet is about $30\,\mathrm{cm}$.
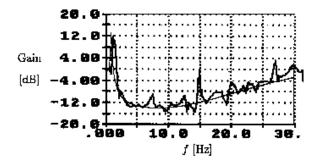

Figure 8: Measured feedback gain (thick line) in the frequency band from 0 to 30 Hz, calculated from the square root of the ratio of the power spectra of simultaneously measured ground motion and magnet jitter. The smooth thinner curve shows the theoretical transfer function [7, 8].

infer the relative beam-beam offset from the orbit of the outgoing bunch [9], Figure 10. Extensive simulation studies have been performed to investigate the capabilities of this scheme. For instance, an initial beam-beam offset of $100\sigma_y$, where σ_y is the vertical rms beam size, can be corrected to zero after 80 bunches (Figure 11), a small number compared to the total number of bunches per train.

Therefore this system is expected to sufficiently reduce ground motion driven luminosity degradation due to beam-beam offset. However, it relies on operation with long bunch trains; during the early commissioning phase, this will not be the case. In contrast, the machine will most likely be started in a single-bunch mode where fast bunch-to-bunch feedback is not possible. Due to the low repetition rate of $f_{\mathrm{rep}} = 5\,\mathrm{Hz}$, uncorrelated motion of the ends of the two linacs around the IR is important even for frequencies
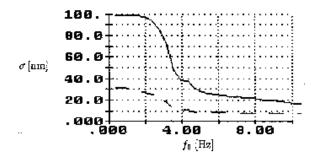

Figure 9: Simultaneosuly measured rms values of ground motion (solid) and magnet motion (dashed) in the frequency band f_{lower} to infinity as function of the lower frequency f_{lower} [7, 8].
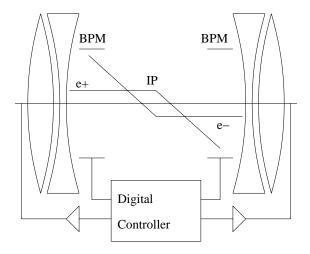

Figure 10: Scheme of the fast bunch-to-bunch orbit feedback system at the IP [9] .

well below $1\,\mathrm{Hz}$. To investigate this experimentally, two seismometers were placed in the two tunnel ends around a HERA interaction region [10]. Data were recorded during quiet and noisy conditions, and the rms relative motion amplitude was calculated by integration of the power spectrum of the difference signal. Figure 12 shows the rms amplitude of relative vertical motion of the two tunnel ends in the frequency range from f_{lower} to infinity as a function of the lower frequency limit f_{lower}. Though the result is certainly dominated by noise in the frequency range below 0.1 Hz, it nevertheless shows that the rms relative vibration amplitude above $f_{\mathrm{rep}}/25 = 0.2\,\mathrm{Hz}$ exceeds the vertical beam size by a large amount. This is confirmed by independent data shown in Figure 13. As a remedy, a relaxed beam optics with larger beam size at the IP needs to be considered during single-bunch commissioning. Another major concern for a Linear Collider is very slow ground motion drift, leading to uncorrelated element misalignment which eventually becomes so large that it affects beam dynamics due to nonlinearities, wakefields, etc. This slow drift is well described by the ATL rule [12], which desribes the relative rms motion amplitude σ_x of two points at a distance L after
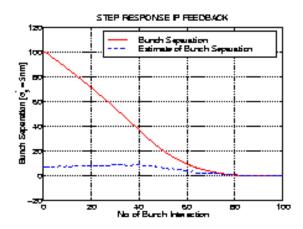
Figure 11: Simulated response of the fast bunch-to-bunch orbit feedback to a stationary $100\sigma_y$ beam separation [9].
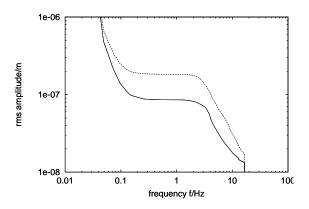

Figure 12: rms relative vertical ground motion amplitudes at a distance of $34\,\mathrm{m}$ in the frequency band from f_lower to $25\,\mathrm{Hz}$ as a function of the lower frequency limit f_lower under quiet (solid) and noisy (dashed) conditions [10].

time T as

$$\sigma_x^2 = A \cdot T \cdot L, \qquad (9)$$

where A is a proportionality constant depending on geological conditions of the particular measurement site.
The proportionality constant A for the DESY site has been calculated from HERA orbit data, Figure 14, as $A = (4 \pm 2) \cdot 10^{-6}\,\frac{\mu\mathrm{m}^2}{\mathrm{Hz}}$ [13].

4   CONCLUSIONS

Ground motion has been studied at DESY for more than a decade, first for the two-ring e-p collider HERA and then for the Linear Collider projects SBLC and TESLA. In spite of rather large ground motion amplitudes caused by the geology of northern Germany and the proximity of the large city of Hamburg, a SBLC or TESLA-type Linear Collider could be operated at DESY. However, active stabilization (SBLC) and/or fast bunch-to-bunch orbit feedback (TESLA) are required. For both compensation schemes, technical solutions have been developed.
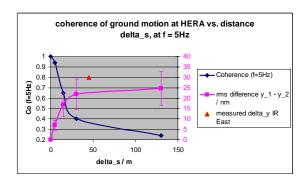

Figure 13: Compilation of coherence of ground motion motion vs. distance data at HERA [11].
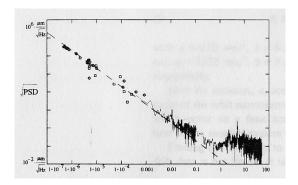

Figure 14: Power spectrum density PSD of vertical orbit motion in HERA, normalized for $\beta = 1\,\mathrm{m}$ [13]. While the (quasi-)continuous spectrum is from the HERA electron ring at $26.6\,\mathrm{GeV}$, the dots are from both HERA-e and HERA-p observations. The proton ring data have been scaled by the FODO cell length to account for the different sensitivities of the lattices.

5   ACKNOWLEDGEMENTS

6   REFERENCES

[1] J. Rossbach, Part. Acc. 23 (1988) 121

[2] C. Montag, J. Rossbach, Ground Vibration, in: A. Chao, M. Tigner, Handbook of Accelerator Physics and Engineering, World Scientific, Singapore, 1999

[3] K. Floettmann, diploma thesis, Hamburg University, 1990

[4] T. O. Raubenheimer, SLAC-387 (1991)

[5] J. Rossbach, M. Lomperski, R. Manukian, C. Montag, DESY M-94-06

[6] V. Shiltsev, B. Baklakov, P. Lebedev, C. Montag, J. Rossbach, DESY HERA 95-06

[7] C. Montag, Nucl. Instr. Meth. A 378 (1996) 369-375

[8] C. Montag, DESY 97-030

[9] I. Reyzl, R. D. Kohaupt, Proc. PAC 1999, New York

[10] C. Montag, Proc. EPAC 2000, Vienna

[11] R. Brinkmann, unpublished

[12] B. Baklakov,   P. Lebedev,   V. Parkhomchuk,   A. Sery, A. Sleptsov, V. Shiltsev, Sov. Phys.ZhTF., Vol. 63, No. 10, 1993 (in Russian)

[13] R. Brinkmann, J. Rossbach, Nucl. Instr. Meth. A 350 (1994) 8-12